Transactions of the Materials Research Society of Japan 25 [2] 525-527 (2000)

Vertical Bridgman Growth of Semiconductor in a Strong Magnetic Field

Yuko Inatomi, Aki Takada and Kazuhiko Kuribayashi
The Institute of Space and Astronautical Science
3-1-1 Yoshinodai, Sagamihara, Kanagawa 229-8510, Japan
Fax: +81-427-59-8461, e-mail: inatomi@materials.isas.ac.jp

Abstract: A formulation of an effective segregation coefficient, K_{eff}, for Bridgman growth of semiconductors in a static magnetic field was derived based on a scaling analysis. The calculated values of K_{eff} for Ga-doped Ge and $Pb_{1-x}Sn_xTe$ crystals agreed well with the experimentally measured ones.

Key words: scaling analysis, vertical Bridgman growth of semiconductor, axial static magnetic field, buoyancy convection

1. Introduction

The quality of semiconductor crystals is mainly influenced by the concentration and distribution of dopants and defects, which are controlled by mass and heat transfer in phases and by interface kinetics. Material transport during growth from liquid phase is caused by thermal and solute convection. The influence of convection on the mass transport is usually evaluated with an effective segregation coefficient, K_{eff}, which is the ratio of the solute concentration in the solid, C_s, to that in the melt [1-4]. According to the model of Scheil [5], C_s can be described as the following function of solidified fraction, f, when the mass transport is influenced by the convection:

$$C_S = K_{eff} C_0 (1-f)^{K_{eff}-1}, \qquad (1)$$

where C_0 is the initial solute concentration in liquid.

If we want to produce a bulk crystal whose concentration profile is homogeneous or intentionally inhomogeneous, K_{eff} should be controlled from an equilibrium segregation coefficient, k_0, to unit along the growth direction by means of damping or acceleration of the convection due to the external force. However, it is difficult to attain to a pure diffusive mass transport state in the liquid during the bulk crystal growth on the terrestrial condition. Therefore, an application of magnetohydrodynamic (MHD) effect of static magnetic field to a conductive fluid is one of the promising methods to damp the convection during Czochralski and Bridgman growths [6-8]. Until now there is few report of simplified but fruitful formulization for the solute concentration distribution in crystals, although a great number of large-scale numerical calculations using computers have been performed to evaluate the distribution in the grown crystal [9, 10].

In the present research, a formulation of the relation between static magnetic induction, B_0, and K_{eff} for vertical Bridgman growth of semiconductors in an axial static magnetic field was derived based on a scaling analysis, and the validity of the estimation was experimentally investigated.

2. Experimental procedure

Ga-doped Ge and $Pb_{1-x}Sn_xTe$ crystals were grown by a vertical single-zone Bridgman method, because the melt of the former material has a higher conductivity and lower density difference between the components than those of the latter. The feed material and the seed crystals were included in a cylindrical quartz-glass ampoule of 8 mm in inner-diameter. To prevent the influence of Marangoni convection on the heat and mass transports in the melt, a quartz-glass rod of 7.5 mmϕ was put on the melt as a rid and it was slightly pushed by quartz-glass wool filled in the ampoule. The ampoule was evacuated up to ~ 10^{-6} mbar, and was subsequently sealed by flame. A mono-ellipsoidal mirror with maximum power of 1 kW was used as heating the feed material. The lamp power of the furnace was controlled by a DC power supply. The growth direction and the vector of the magnetic induction were parallel to the gravity vector. The other growth conditions and the physical properties of the materials were shown in Table 1. An axial static magnetic field in the liquid zone of the ampoule, B_0, was produced by a liquid helium free superconducting magnet. The magnet had a large bore 300 mm in diameter and 600 mm in length and was designed to generate a homogeneous magnetic field with maximum induction of 6 T at the center. The furnace was mounted into the bore. Figure 1 shows the experimental configuration.

After growth, the samples were cut along the growth directions using a thin wheel with diamond particles, and polished mechanically to be mirror surfaces. The concentration profiles in the crystals were characterized by a four point probe method and an EDX for Ga-doped Ge and $Pb_{1-x}Sn_xTe$, respectively.

3. Scaling analysis

The influence of the buoyancy force on the heat and mass transport phenomena in the fixed-coordinate system was studied based on scaling analyses. Friedrich *et al.* [11] modified the scaling analysis [12] to estimate the fluid behavior on the centrifuge, where the centrifugal force and the Coriolis force were taken into account. In the present research, the analysis was applied to the MHD problem under a static magnetic field instead of Coriolis force based on the Friedrich's procedure.

The Navier-Stokes equation for an incompressible fluid in the Boussinesq approximation, the continuity equation, and the governing equations of heat and mass transport can be written as follows:

$$(\partial \mathbf{u}/\partial t) + (\mathbf{u}\cdot\nabla)\mathbf{u} = -(1/\rho_0)\nabla P + \nu\nabla^2\mathbf{u} + \mathbf{F}, \qquad (2a)$$

$$\mathbf{F}=\{\beta(T-T_0)+\alpha(C-C_0)\}\mathbf{g} -(\sigma/\rho_0)\{(\mathbf{u}\times\mathbf{B})\times\mathbf{B}\}\ , \quad (2b)$$

$$\nabla\cdot\mathbf{u}=0\ , \quad (3)$$

$$(\partial T/\partial t)+\mathbf{u}\cdot\nabla T=\kappa\nabla^2 T, \quad (4)$$

$$(\partial C/\partial t)+\mathbf{u}\cdot\nabla C=D\nabla^2 C. \quad (5)$$

When the curl operators were applied to Eqs. (2a) and (2b), the following equations for the steady state condition of the fields were derived:

$$\nu\nabla\times\{\nabla\times(\nabla\times\mathbf{u})\}+\nabla\times\{(\mathbf{u}\cdot\nabla)\mathbf{u}\}-\nabla\times\mathbf{F}=\mathbf{0}\ , \quad (6a)$$

$$\nabla\times\mathbf{F}= \mathbf{g}\times(\beta\nabla T+\alpha\nabla C)-(\sigma/\rho_0)\nabla\times\{(\mathbf{u}\times\mathbf{B})\times\mathbf{B}\}\ . \quad (6b)$$

The radius of the liquid phase, r, and the unknown velocity, u_r, were introduced as the characteristic length and flow velocity into Eqs. (6a) and (6b). The differential operator, the flow velocity, the buoyancy and Lorentz forces, and the gravity vector were respectively normalized by the absolute values as follows:

$$(\nu u_r/r^3)\hat{\nabla}\times\{\hat{\nabla}\times(\hat{\nabla}\times\hat{\mathbf{u}})\} +(u_r^2/r^2)\hat{\nabla}\times\{(\hat{\mathbf{u}}\cdot\hat{\nabla})\hat{\mathbf{u}}\}-|\nabla\times\mathbf{F}|(\hat{\nabla}\times\hat{\mathbf{F}})\approx 0\ , \quad (7a)$$

$$\hat{\nabla}\equiv r\nabla\ ,\ \hat{\mathbf{u}}\equiv\mathbf{u}/u_r\ ,\ |\hat{\nabla}|=|\hat{\mathbf{u}}|=1\ . \quad (7b)$$

The radius temperature and concentration gradients were assumed to be proportional to the product of the interface gradient against the growth direction, m, and the axial temperature and concentration gradients in the vicinity of the solid/liquid interface, G_T and G_C, respectively. Therefore, the following approximation were applied to the buoyancy term in Eq. (6b):

$$|\mathbf{g}\times\nabla T|\approx mg_0 G_T\ ,\ |\mathbf{g}\times\nabla C|\approx mg_0 G_C\ . \quad (8)$$

The relative importance of the body forces on u_r in Eq. (7a) can be given by the dimensional coefficients in front of the normalized vector terms which should be on the order of unit:

$$(\nu u_r/r^3)+(u_r^2/r^2)-mg_0(\beta G_T+\alpha G_C) +(\sigma u_r B_0^2/\rho_0 r)\approx 0\ , \quad (9)$$

From Eq. (9), Reynolds number, Re, was derived by Hartmann number, Ha, and thermal and solutal Grashof numbers, Gr_T and Gr_S:

$$Re^2+(1+Ha^2)Re\approx|m(Gr_T+Gr_S)|\ . \quad (10)$$

The solution of Eq. (10) for Re was given by:

$$Re\approx-(1+Ha^2)/2+\sqrt{(1+Ha^2)^2/4+|m(Gr_T+Gr_S)|}\ , \quad (11)$$

where the requirement Re > 0 was taken into consideration.

According to the model of Ostrogorsky and Müller [13], the relation between K_{eff} and the segregation parameter, Δ, was:

$$K_{eff}=k_0/\{1-(1-k_0)\Delta\}\ , \quad (12)$$

where (a) Δ = 1: pure diffusive mass transport, and (b) Δ = 0: strong convective mass transport. At low Gr_S and Gr_T, the normalized solute boundary layer thickness in the melt, X_C^*, can be regarded as a constant value, $D/(rV_G)$ where V_G is the growth rate. Introducing of Schmidt number, Sc, Peclet number, Pe, X_C^*, and Re yields Δ as [11]:

$$\Delta=\{1+ScX_C^*Re/(6Pe)\}^{-1}\ , \quad (13)$$

where the velocity profile was approximated as linear.

In the result, K_{eff} can be simply estimate from the experimental condition, the physical properties of the materials, and Eqs. (11-13).

4. Results and discussion

Figure 2 shows the normalized solute concentration profiles in the grown crystals versus f in Eq. (1) for Ga-doped Ge and $Pb_{1-x}Sn_xTe$. In the case of Ga-doped Ge, the mass transport in the Ge melt attained to the diffusive regime at B_0 = 6 T, whereas the transport was governed by strong mixing due to the convection at B_0 = 0 T. The Lorentz force in the melt was thought to be obviously effective to damp the convection due to the weak buoyancy force and the large conductivity in the melt. On the other hand, the solute transport was strongly governed by the convection at B_0 = 0 T and 6 T for $Pb_{1-x}Sn_xTe$, and therefore the Lorentz force in the melt was weak to damp the convective flow contrast with the case of the Ga-doped Ge.

The estimated K_{eff}'s based on Eqs. (11-13) were shown in Fig. 3, and we can see the values agreed well with the experimental ones which were calculated by the following equation:

$$K_{eff}=1-[(dCs/df)/(2Cs)]_{f=0.5} \quad (14)$$

It was concluded that the formulation of K_{eff} as a function of B_0 derived from the scaling analysis was effectual to estimate the concentration profile in the grown crystal.

5. Conclusion

An effective segregation coefficient for a vertical Bridgman growth of semiconductors in an axial static magnetic field was derived based on a scaling analysis. The calculated values of the coefficients for Ga-doped Ge and $Pb_{1-x}Sn_xTe$ crystals agreed well with the experimentally measured ones from 0 to 6 T of the magnetic induction.

Nomenclature

$\mathbf{g}$	vector of acceleration of gravity
g_0	$\|\mathbf{g}\|$, 9.81 m/s^2
P	pressure
T	temperature
u_r	characteristic velocity in liquid
κ	thermal diffusivity
Pr	Prandtle number, ν/κ
Sc	Schmidt number, ν/D
Re	Reynolds number, $u_r r/\nu$
Ha	Hartmann number, $B_0 r(\sigma/\rho_0\nu)^{1/2}$
Gr_T	thermal Grashof number, $\beta G_T g_0 r^3/\nu^2$
Gr_S	solute Grashof number, $\alpha G_C g_0 r^3/\nu^2$

Acknowledgement

This work was supported by a grant from Japan Space Forum (Contract No. 9JSF-283).

References

[1] J.A. Burton, R.C. Prim and W.P. Slichter, *J. Chem. Phys.* **21** (1953) 1987.

[2] F. Rosenberger, *Fundamentals of Crystal Growth I*, (Springer, Berlin, 1979).

[3] G. Müller, in: *Crystals: Growth, Properties and Applications*, Vol. 12 (Springer, Berlin, 1988).
[4] L.O. Wilson, *J. Crystal Growth* **44** (1978) 247.
[5] E. Scheil, *Z. Metallk.*, **34** (1942) 70
[6] K. Terashima, T. Katsumata, F. Orito, T. Kikuta, T. Fukuda, *Japan J. Applied Phys.* **22** (1983) L323.
[7] C.H. Su, S.L. Lehoczky and F.R. Szofran, *J. Crystal Growth* **109** (1991) 392.
[8] R.W. Series and D.T.J. Hurle, *J. Crystal Growth* **113** (1991) 305.
[9] R. Bessaih, M. Kadja, Ph. Marty, *Int. J. Heat and Mass Transfer* **42** (1999) 4345.
[10] D.H. Kim, P.M. Adornato and R. A. Brown, *J. Crystal Growth* **89** (1988) 339.
[11] J. Friedrich, J. Baumgartl, H.-J. Leister, and G. Müller, *J. Crystal Growth* **167** (1996) 45.
[12] D. Camel and J.J. Favier, *J. Physique* **47** (1986) 1001.
[13] A.G. Ostrogorsky, G. Müller, *J. Crystal Growth* **121** (1992) 587.

Table 1. Physical properties of the melt and the experimental condition.

		Ga_xGe_{1-x}			$Pb_{1-x}Sn_xTe$
Initial concentration, C_0	at.%	0.1	0.2	1	20
Electrical conductivity, σ	1/Ω•m	1.5×10^{6}			1.6×10^{5}
Equilibrium segregation coefficient, k_0		8.7×10^{-2}	8.7×10^{-2}	6.1×10^{-2}	0.58
Solute expansion Coefficient, α	1/at.%	-7.3×10^{-4}			-2.3×10^{-3}
Thermal expansion Coefficient, β	1/K	1.1×10^{-4}			1.1×10^{-4}
Kinematic viscosity, ν	m^2/s	1.4×10^{-7}			2.8×10^{-7}
Density of solution, ρ_0	kg/m^3	5.5×10^{3}			7.8×10^{3}
Diffusion coefficient, D	m^2/s	1.9×10^{-8}			5.3×10^{-9}
Concentration gradient, G_C	at.%/m	-40	-80	-400	-3.8×10^{3}
Temperature gradient, G_T	K/m	3.0×10^{3}			3.0×10^{3}
Gradient of interface from planarity, m		0.12			0.36
Growth rate, V_G	m/s	8.3×10^{-6}			2.2×10^{-6}
Melt radius, r	m	4.0×10^{-3}			
Magnetic induction, B_0	T	0.0 ~ 6.0			

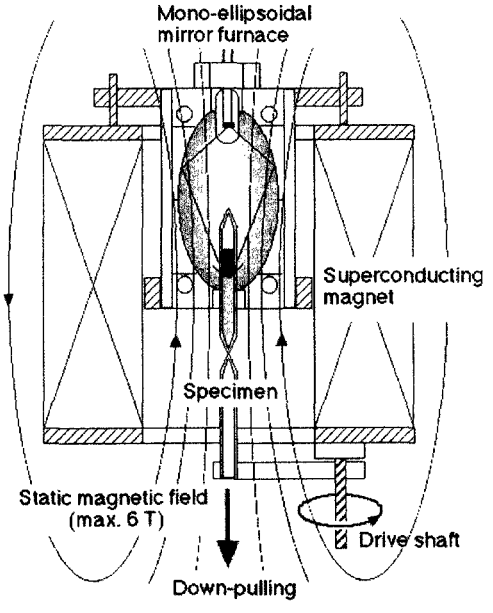

Fig. 1. Schematic drawing of the experimental setup.

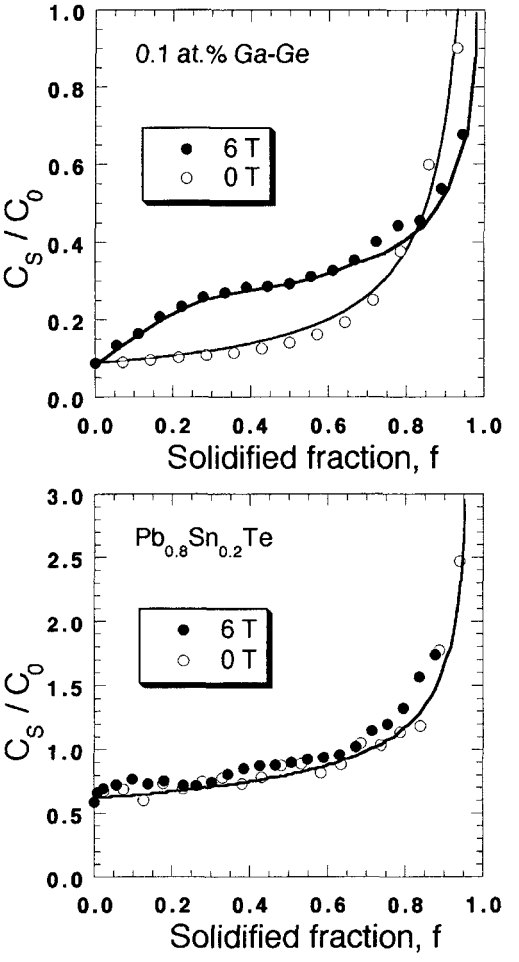

Fig. 2. Normalized concentration profile in the crystal, C_S/C_0, along the growth direction. C_0 is the initial concentration in the melt.

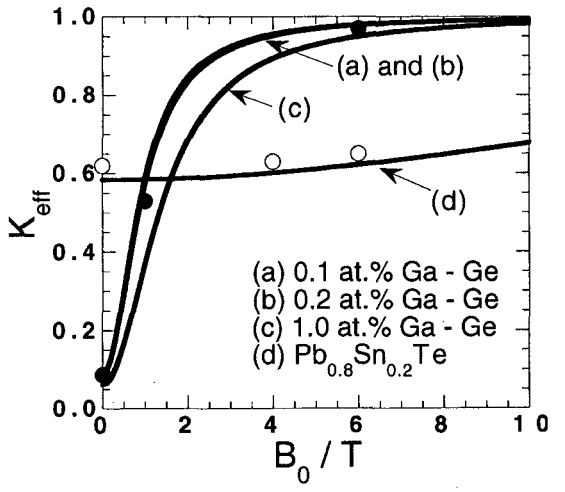

Fig. 3. Calculated K_{eff} as a function of magnetic induction, B_0. The marks, ● and ○, correspond to the experimental values for Ga_xGe_{1-x} (x = 0.002) and $Pb_{0.8}Sn_{0.2}Te$.

(Received January 26, 1999; accepted February 24, 2000)